Research Statement

Jonathan Klamkin
University of California Santa Barbara

Our group conducts pioneering research in ***integrated photonic technologies for communications and sensing applications***. We are a ***vertically integrated research group*** in that we conduct fundamental materials research, fabricate devices and photonic integrated circuits (PICs), and build and characterize electronic-photonic integrated subsystems. My personal objective is to impact extremely challenging problems that can be addressed with integrated photonic technologies, while training, educating, and inspiring students and researchers. Our group has been fairly productive, having published more than 70 papers in the last two years. In the same period, I have given 30 invited talks, including one plenary. As described below, our research has broad reach covering many applications including microwave photonics and wireless communications, free space optical communications, lidar gas sensing, data center communications, and beam steering. The following summarizes some of our primary research areas.

1. Integrated microwave photonics for millimeter wave communications and phased arrays

Broadband optical beam forming networks (OBFNs) are key for future photonics-assisted wideband wireless communications and phased arrays. Optical phase shifters can replace traditional RF phase shifters to perform beam steering of an RF signal, however, beam-squint limits the bandwidth. True time delay (TTD) is an enabling technology for optical signal processing functions in microwave photonics, particularly in OBFNs for photonics-enabled signal generation with squint-free beam steering capability. Use of PICs is desirable for OBFNs owing to the large available bandwidth and for compactness, low loss, and precise waveguide length control. We have developed ***key PIC TTD technologies based on optical ring resonators (ORRs) and switched delay lines (SDLs)***. In addition to deriving novel implementations of these technologies in ***ultra-low loss silicon nitride waveguides***, we have developed automated measurement techniques to characterize and calibrate their delay properties, ***and for the first time, employed optical TTDs in integrated OBFNs for beam steering of millimeter wave signals***. Our systematic approach enables ***programmable multi-functional PICs for microwave photonics***.

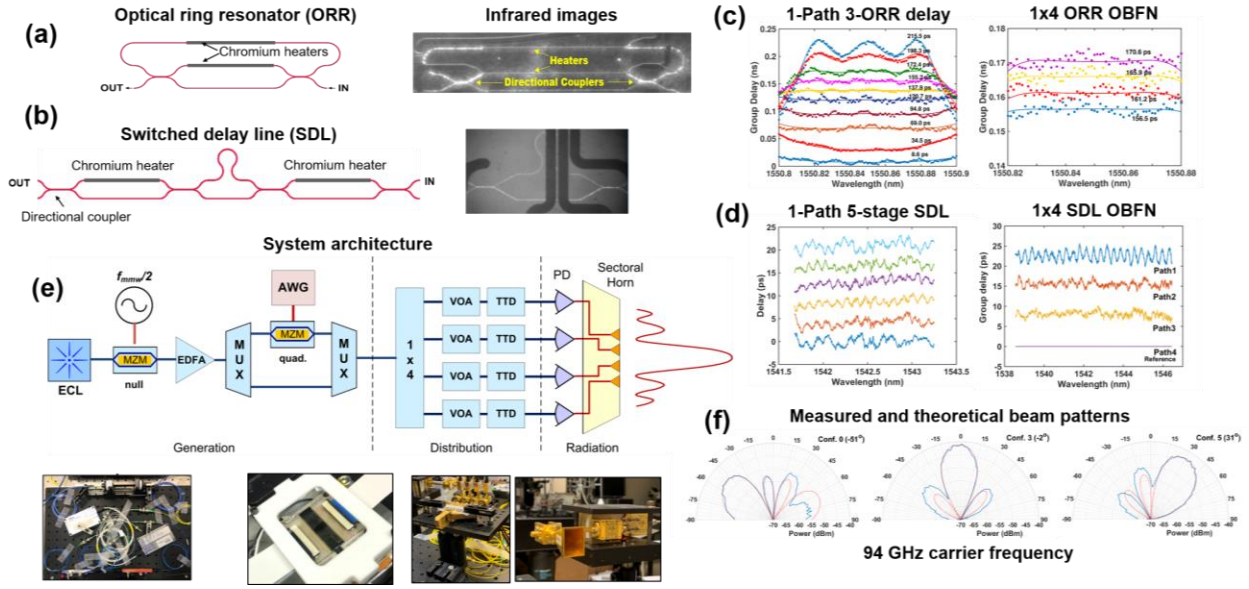

Fig. 1. Schematics and infrared images (with light propagating in waveguides) of (a) ORR and (b) SDL TTD elements. (c) Group delay tuning characteristics for a 3-ORR single path delay demonstrating ~200 ps tuning along with corresponding programmed 1x4 OBFN with fixed delay difference for adjacent paths. (d) Tuning characteristics for a 5-stage SDL along with corresponding programmed 1x4 OBFN with fixed delay difference for adjacent paths. (e) System architecture including photographs of various stages (second photograph is a packaged 1x4 OBFN chip). (f) Measured and theoretical beam patterns for 94 GHz carrier frequency.

Figure 1(a) and (b) show schematics and infrared images of single elements of ORR and SDL TTDs, respectively. Each ORR incorporates micro-heaters for independent control of the ring coupling and resonance frequency. Cascaded ORRs (three in each path) are implemented to allow for wider bandwidth delay tuning. Custom low-noise current controllers were developed to tune all of the heaters, and a tuning algorithm was employed to program the delay spectrum by measuring it in real time and fitting to a theoretical curve. The delay is programmed to address the tradeoffs between total delay tuning range, bandwidth, and delay ripple (Fig. 1(c)). In comparison, the SDL-based TTD achieves extremely broad bandwidth. However, because Mach-Zehnder switches are imperfect (i.e. do not achieve perfect 50:50 splitting), some delay ripple is induced when a switch is programmed in the cross state, and this delay ripple will not only accumulate as progressing through stages, but also worsen should other switches in the chain be programmed in the cross state as well. To overcome this, we devised a novel SDL architecture that limits the number of crosses to minimize delay ripple (Fig. 1(d)). Finally, ***we constructed an entire system to generate, distribute, and emit a beam-steerable millimeter wave (94 GHz) signal*** (Fig. 1(e)). Figure 1(f) shows some examples of emitted beams steered to various emission angles. As shown, there is a close match between the measured and theoretical beam patterns. This represents the ***first ever reported demonstration of millimeter wave beam steering with an integrated OBFN***. This work has been supported by the Department of Defense (through a collaboration with Johns Hopkins University Applied Physics Laboratory) and by the NASA Space Technology Mission Directorate. More details can be found in the references provided below.

References

[1] J. Capmany, et al., IEEE Microwave Magazine, vol. 16, no. 8, 2015.
[2] J. A. Nanzer, et al., FIO, vol. 34, no. 4, 2015.
[3] Y. Liu, et al., JSTQE vol. 24, no. 4, 2018.
[4] Y. Liu, et al., JLT vol. 35, no. 22, 2017.
[5] Y. Liu, et al., CLEO, SF3N.6, 2019.
[6] Y. Liu, et al., OFC, Th1C.5, 2019.
[7] Y. Liu, et al., IPR, ITh3B. 4, 2018.
[8] Y. Liu, et al., Proc. SPIE 10531, 2018.
[9] Y. Liu, et al., MWP, pp. 1-4, 2017.
[10] Y. Liu, et al., IPR, IW2A.2, 2017.
[11] Y. Liu, et al., IMS, pp. 443-446, 2017.
[12] Y. Liu, et al., MWP, pp. 321-324, 2016.
[13] Y. Liu, et al., IPR, IW1B.3, 2016.

2. III-V on silicon heteroepitaxy for photonics and electronics applications

Our group has developed expertise in novel compound semiconductor crystal growth techniques for both photonics and electronics applications. In addition to growing materials for state-of-the-art indium phosphide (InP) and gallium arsenide (GaAs) PIC platforms, we have developed ***innovative technologies for growth of group III-V materials on silicon and have demonstrated record quality***, considering threading dislocation density (TDD) and surface smoothness. To address the challenges of growing III-V materials on silicon, we have leveraged the benefits of metalorganic chemical vapor deposition (MOCVD) for selective area nonplanar growth. We optimized growth conditions for GaAs on V-groove silicon (GoVS) and strained layer superlattices (SLSs), which assist to eliminate the formation of anti-phase boundaries and to filter defects, respectively. Figure 2(a) and (b) summarize development of GoVS templates with SLSs and inclusion of thermal cycle annealing (TCA), that latter of which furthers TDD reduction. As revealed by electron channel contrast imaging (ECCI) analysis, the TDD reduction evolves during the various stages of this template growth. With only two SLSs, the TDD achieved is as low as 9.1×10^6 cm^{-2}. This can be further lowered with additional SLSs and optimization, but already represents the state of the art. Additionally, we have developed high quality indium arsenide (InAs) quantum dots (QDs) since they are believed to be less sensitive to defects than quantum wells. Figure 2(c)-(e) show cross section transmission electron microscopy (TEM) images of a multi-layer QD active region grown on a GoVS template comprising two SLSs.

Figure 2(f) shows the layer structure for a QD calibration sample and Fig. 2(g) a corresponding atomic force microscopy (AFM) image of the QDs demonstrating excellent size, shape, density, and uniformity. Close-up TEM images of the QDs are shown in Fig. 2(h) and (i). Lastly, Fig. 2(j) shows photoluminescence (PL) measurement results, comparing a QD active region grown on a native GaAs substrate to that grown on a GoVS template. The PL intensity and linewidth are nearly identical for both, indicating that ***we have achieved extremely high quality GaAs template material on on-axis (001) CMOS-compatible silicon and***

shown that QDs appear to be effectively less sensitive to defects. In addition to InAs QD lasers on silicon for the 1310-nm wavelength region, we have also developed ***record low defect density InP on silicon templates, novel nano-scale lasers on silicon on insulator (SOI), and novel pseudo-substrate techniques based on selective area growth***. Primarily for low-energy transistor applications, we have developed ***novel confined lateral growth techniques to realize lateral triple heterojunctions for tunnel field effect devices***. Further details are provided in the references below. This work has been supported by AFRL through AIM Photonics, by DARPA, and jointly by the NSF and SRC.

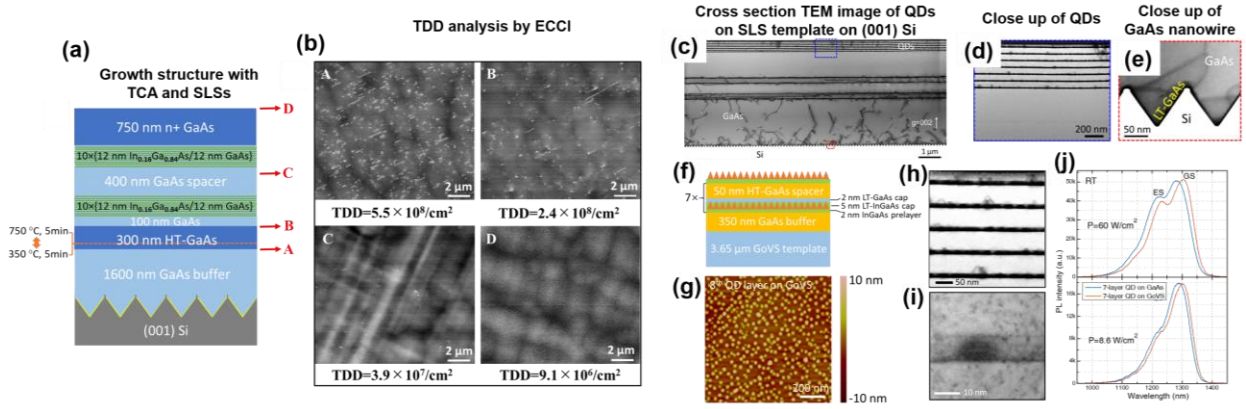

Fig. 2. (a) Layer structure for GoVS template with SLSs and (b) corresponding ECCI analysis. (c), (d) TEM images of QDs on GoVS template. (e) TEM image of GaAs in V-groove. (f) QD calibration structure and (g) corresponding AFM image. (h), (i) Close-up TEM images of QDs. (j) PL measurements at different pump powers for QDs grown on native substrate and on GoVS template.

References

[1] B. Shi, et al., APL, vol. 114, no. 17, 2019.
[2] B. Shi, et al., CSW, paper ThA2-4, 2019.
[3] L. Wang, et al., CLEO, paper JTu2A.82, 2019.
[4] S. Suran Brunelli, et al., JAP, 2019.
[5] B. Shi, et al., OMVPE-19, 2019.
[6] J. Klamkin, et al., BCICTS, 2018.
[7] S. Suran Brunelli, et al., TECHNON, 2019.
[8] J. Klamkin, et al., IPR, 2019.
[9] L. Megalini, et al., CLEO, paper AMA4A.6, 2017.
[10] L. Megalini, et al., IPR, paper ITu2A.3, 2017.
[11] L. Megalini, et al., APL, vol. 111, no. 3, 2017.
[12] L. Megalini, et al., Materials, vol. 11, no. 3, 2018.
[13] L. Megalini, et al., JEM, vol. 47, no. 2, 2018.
[14] L. Megalini, et al., CSW, 2018.
[15] S. Suran Brunelli, et al., CSW, 2018.
[16] S. Suran Brunelli, et al., ICMOVPE, 2018.

3. High-power photonic integrated circuits and free space optical communications

Free space optical communications has gained significant attention recently due to the demand for high data rate communications in space (see Fig. 3(a)). In addition to several demonstrations and ongoing programs at various space agencies, the commercial sector (including tech giants such as SpaceX, Amazon, Facebook, Google, and others) has been pursuing "space networks" to deliver broadband access to the developing world, to provide internet access to more commercial flights, to provide connectivity during and following disasters, and to enable high resolution imagery and video from space on demand. ***PICs, which are inherently low cost, size, weight and power (CSWaP), are ideal for free space communications to enable high data rate links on small satellite platforms (i.e. CubeSat) that are much lower in cost and deploy more frequently***.

For free space optical communications, transceivers typically utilize power-efficient, in contrast to spectrally-efficient, modulation formats. Higher optical output power is also desired, and space qualification is required. Our group has been pioneering the development of high-performance PICs for this application. In addition to adapting transmitter for various modulation formats (on-off keying (OOK), differential phase shift keying (DPSK), pulse position modulation (PPM)), we have developed a ***high-power InP PIC platform currently capable of nearly 250 mW of optical output power***. Figure 3(b) shows an image of a fabricated InP transmitter that includes a tunable laser, semiconductor optical amplifiers (SOAs), and a high-speed modulator. Figures 3(c)-(e) summarize the performance of the integrated laser,

and Fig. 3(f) the modulation characteristics up to 20 Gbps. Figure 3(g) describes the high-power SOA concept that was incorporated into this platform. Within an SOA, the mode size is increased both horizontally and vertically to achieve a significantly larger modal area capable of much higher output power (see Fig. 3(h)). Additionally, we have developed an electronic-photonic integrated transmitter for DPSK. This modulation format is desirable because it leverages phase modulation at the transmitter but can utilize a simplified non-coherent delay interferometer based detection at the receiver. Figure 3(i) shows photographs of the DPSK PIC on carrier integrated with a custom driver board, and Fig. 3(j) summarizes the modulation capabilities of this transmitter. This work has been supported through various NASA programs including an Early Career Faculty Award, an Early Stage Innovations Award, and STTR programs with Freedom Photonics.

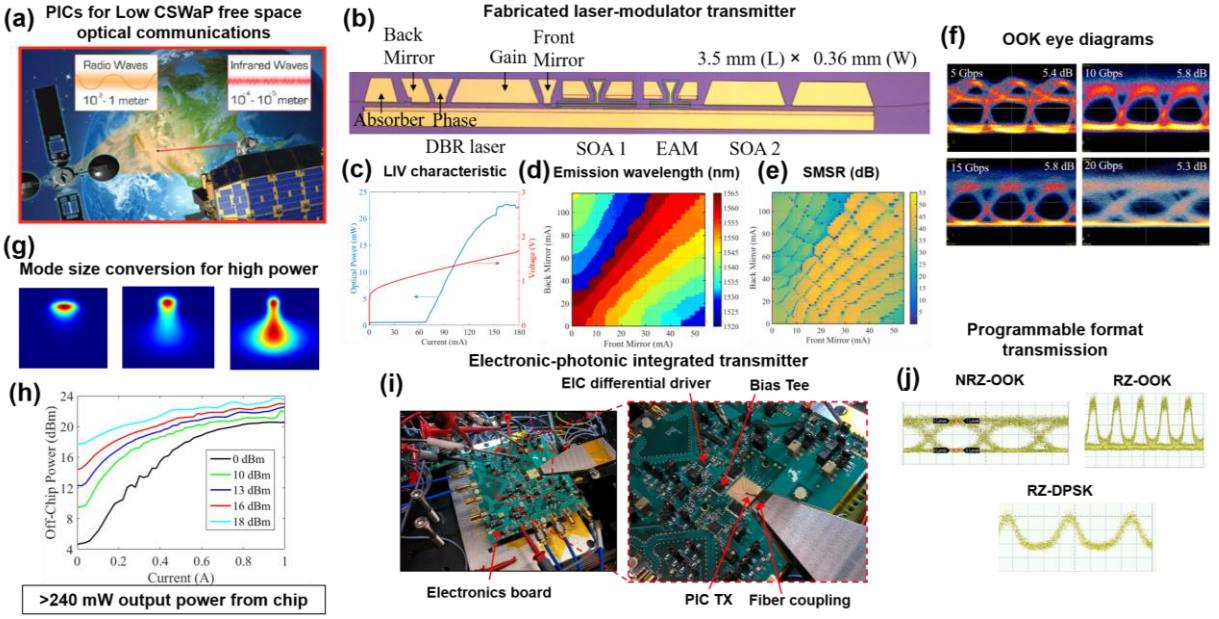

Fig. 3. (a) Illustration of free space optical communications. (b) Microscope image of InP PIC transmitter with corresponding (c) light-current-voltage (LIV) characteristic, (d) wavelength tuning map, (e) side mode suppression ratio (SMSR) map, and (f) OOK eye diagrams for 5, 10, 15, and 20 Gbps operation. (g) Illustration of mode size conversion for increasing power handling of PIC platform and (h) corresponding high-power SOA measurements demonstrating greater than 240 mW output power. (i) Photographs of electronic-photonic integrated transmitter for RZ-DPSK transmission and (j) corresponding eye diagrams for NRZ-OOK, RZ-OOK, and RZ-DPSK modulation.

References

[1] J. Klamkin, et al., BCICTS, 2018
[2] H. Zhao, et al., JSTQE, vol. 25, no. 6, 2019.
[3] H. Zhao, et al., JSTQE, vol. 24, no. 6, 2018.
[4] H. Zhao, et al., ISLC, paper MC.5, 2018.
[5] H. Zhao, et al., CLEO, paper JW2A.52, 2018.
[6] H. Zhao, et al., IPR, paper ITu4B.6, 2018.
[7] J. Fridlander, et al., SPIE LASE, 1091026, 2019.
[8] J. Fridlander, et al., CLEO, 2018.
[9] M. Krainak, et al., SPIE LASE, 108990F, 2019.
[10] M. Krainak, et al., IPC, 2018.

4. Integrated photonics for remote Earth science sensing lidar

Building on our work in PICs for free space optical communications, we have been collaborating with NASA Goddard Space Flight Center (GSFC) to develop ***PICs for remote Earth science sensing lidar, specifically for carbon dioxide (CO_2) detection***. GSFC has spent several years developing an atmospheric CO_2 sensor based on laser spectroscopy that uses a tunable laser to scan through a CO_2 gas absorption line centered at 1572 nm. The current laser transmitter uses mature technologies and meets all the optical performance requirements but is relatively bulky and inefficient. UCSB and GSFC have initiated a program to significantly improve the implementation for a resource constrained space-flight mission platform by leveraging a PIC solution.

As shown in Fig. 4(a)-(c), the seed laser being developed is a pulsed laser with tunable wavelength output. Consecutive pulses are emitted at different wavelengths that step across the absorption feature of interest. The wavelength of each pulse is individually locked to an exact value. This is achieved by using a master laser locked to the center of the CO_2 absorption as an absolute reference and using offset locking to tune a slave laser by means of an optical phase-locked loop (OPLL). The PIC solution will significantly reduce system CSWaP allowing for frequent deployment on small platforms (see Fig. 4(d) and (e)). For the PIC solution, a distributed feedback (DFB) laser is being utilized for the master and a sample grating distributed Bragg reflector (SGDBR) laser for the slave. A fully fabricated PIC is shown in Fig. 4(f) along with laser tuning characteristics in Fig. 4(g) and (h). ***This is the first time that a stable DFB laser was monolithically integrated with a widely tunable DBR laser; such a capability is beneficial for sensing applications***. This work is currently being supported by NASA.

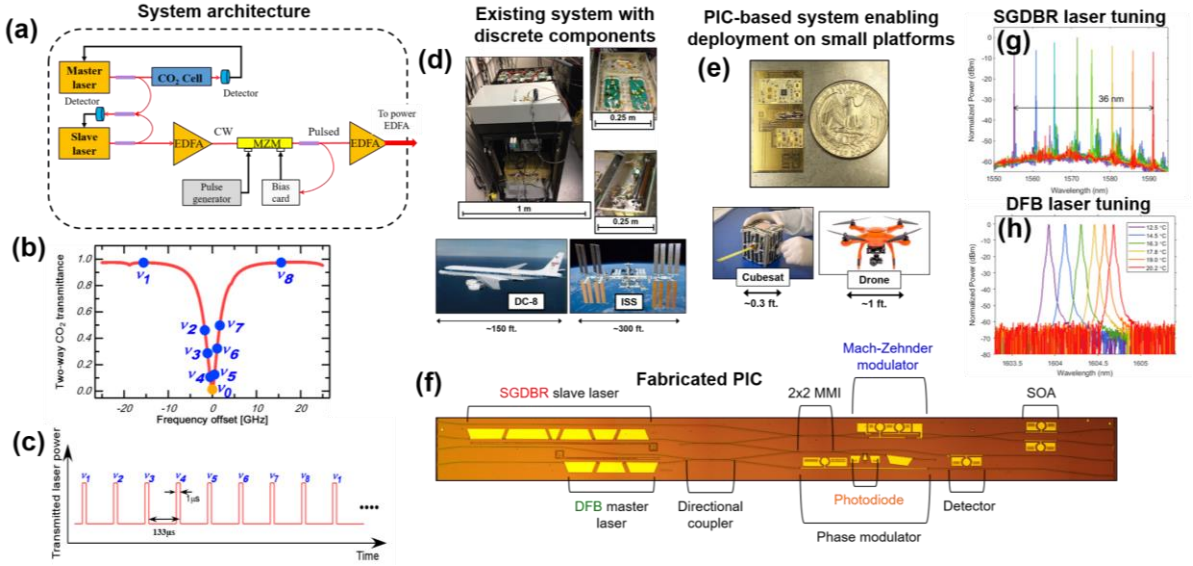

Fig. 4. (a) System architecture. (b), (c) CO_2 absorption line and measurement description. (d), (e) Illustration of benefits of integration to reduce system CSWaP and enable deployment on small space platforms. (f) Photograph of fabricated PIC. (g), (h) Laser tuning spectra for SGDBR and DFB lasers fabricated on same chip.

References

[1] S. R. Kawa, et al., Tellus B, vol. 62, 2010.
[2] J. Klamkin, et al., BCICTS, 2018
[3] V. Rosborough, et al., IPR, 2019.
[4] K. Numata et al., Opt. Express, vol. 20, 2012.
[5] J. Klamkin, et al., ESTF, 2018.
[6] J. Fridlander, et al., ESTF, 2019.

5. Integrated nanophotonics and metasurfaces

We have developed ***reconfigurable metasurfaces based both on indium tin oxide (ITO), and more recently, indium silicon oxide (ISO)***. These metasurfaces consist of nano-scale metallic resonator arrays fabricated on metal-insulator-metal (MIM) multi-layer structures. Light can be strongly coupled at a metal-dielectric interface, enabling subwavelength optical components that overcome the diffraction limit. ***Metasurfaces allow for manipulation of the light amplitude, phase, and polarization, enabling a wide range of applications including optical antennas, modulators, beam steering devices for lidar and communications, solar cells, and bio-sensing***.

To enable active tuning, we incorporated electro-optic tunable materials into metasurfaces, and these materials were embedded in MIM plasmonic cavities. In this way, a gate bias can be applied for tuning. Transparent conducting oxides (TCOs) such as ITO and ISO are attractive because they are CMOS compatible and simple to fabricate. Figure 5 summarizes our recent work on realizing gate-tunable metasurfaces based on ISO. Devices with various size (width and pitch) metal rods were fabricated (Fig. 5(b)-(e)). Figure 5(f) shows the simulated reflectance for a resonator period of 1 μm with resonance wavelengths for the various devices marked. Figure 5(g)-(i) compare 3D finite element method (FEM) simulations to Fourier transform infrared (FTIR) spectroscopy measurements and Fig. 5(j)-(m) show the

electric field profiles for device D1 at a wavelength of 2 µm, device D2 at 2.45 µm, device D3 at 1.7 µm and D3 at 6.05 µm, respectively. Lastly, Fig. 5(n) and (o) illustrate an experimental demonstration of active tuning for device D1 where the resonance wavelength was shifted by 50 nm and a reflectance change of 33% was demonstrated. These results are promising for high efficiency gate-tunable metasurface applications and future work will build 2D arrays of such devices for beam steering applications. This work is being performed in collaboration with Boston University.

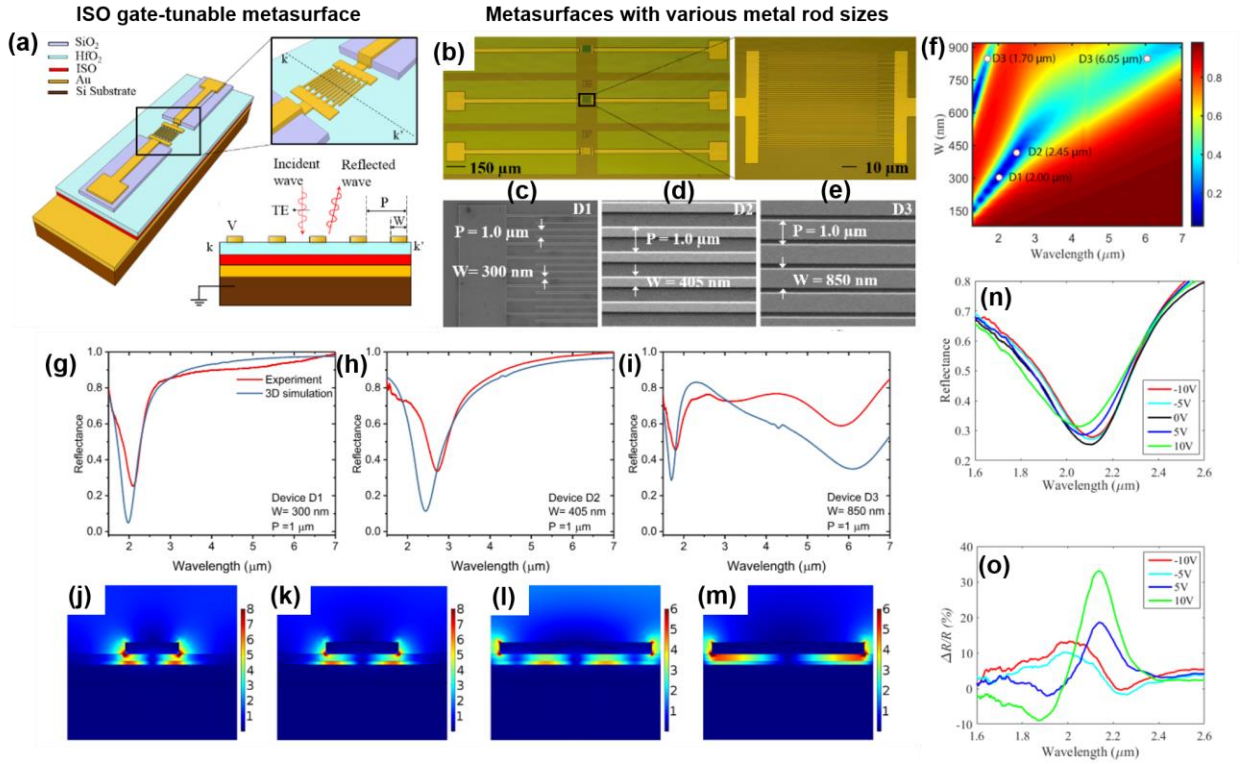

Fig. 5. (a) ISO metasurface device. (b)-(e) Microscope and SEM images of devices with various metal rod geometries. (f) Simulated reflectance map. (g)-(i) Comparison of FEM simulations to FTIR measurements showing good agreement. (j)-(m) Simulated electric field profiles. (n), (o) Illustration of gate tunable metasurface.

References

[1] H. Zhao, et al., Nanophotonics, 2019 (submitted).
[2] H. Zhao, et al., JSTQE, vol. 21, no. 4, 2015.
[3] H. Zhao, IPR, 2019.
[4] H. Zhao, et al., IPC, paper TuH3.3, 2014.
[5] H. Zhao, et al., IPR, paper JM3B.4, 2014.
[6] W. A. Britton, et al., APL, vol. 114, no. 16, 2019.